AN ABSTRACT OF THE THESIS OF

LETA ANDREWS (Name) for the degree MASTER OF SCIENCE (Degree)

in ATMOSPHERIC SCIENCES (Major Department) presented on October 23, 1974 (Date)

Title: A STATISTICAL STUDY OF THE CORRELATION BETWEEN THE SURFACE AND SURFACE GEOSTROPHIC WINDS IN THE WILLAMETTE VALLEY

Redacted for privacy

Abstract approved: Larry J. Mahrt

Relationships among the surface wind, horizontal synoptic-scale pressure gradient and topography are studied in the Willamette Valley in western Oregon. Terrain features alter the standard surface wind-pressure gradient relationship such that the angle between the surface wind and the surface geostrophic wind is most frequently 60°.

In winter the surface flow is predominantly southerly and surface geostrophic flow varies from southerly to westerly. Little diurnal change occurs in the average surface wind, the average surface geostrophic wind and their relationship with each other because the air in the valley is generally stably stratified throughout the day.

Partially in response to the northward extension of the sub-tropical anticyclone summertime surface winds and surface geostrophic winds are northerly, except during afternoon episodes of

marine air invasion when surface winds are westerly. The pressure gradient is 88% less intense in summer but the ratio of the magnitudes of the surface wind and surface geostrophic wind, R, is 125% greater than in winter. However, a sharp summertime morning maximum in R of -0.67 is diminished by early afternoon as differential surface heating establishes a strong afternoon pressure gradient.

When the surface geostrophic wind vector is cross-valley, the surface wind is still most frequently parallel to the valley and the surface geostrophic wind speed is largest and most variable.

Because of the importance of terrain and meso-scale events, little correlation between the surface winds and synoptic-scale pressure gradient is found.

A Statistical Study of the Correlation Between the Surface and Surface Geostrophic Winds in the Willamette Valley

by

Leta Andrews

A THESIS

submitted to

Oregon State University

in partial fulfillment of
the requirements for the
degree of

Master of Science

Completed October 23, 1974

Commencement June 1975

APPROVED:

Redacted for privacy

Assistant Professor of Department of Atmospheric Sciences

in charge of major

Redacted for privacy

Chairman of Department of Atmospheric Sciences

Redacted for privacy

Dean of Graduate School

Date thesis is presented October 23, 1974

Typed by Clover Redfern for Leta Andrews

ACKNOWLEDGMENTS

I wish to express my appreciation to Dr. Larry J. Mahrt, my major professor, for suggesting this topic and for his guidance during the course of this study.

I especially wish to thank Mr. Joseph Hennessey, Jr. for his encouragement and many helpful suggestions throughout the course of my study and Drs. Richard Boubel, Fred Decker, Erwin Berglund, E. Wendell Hewson, David Barber and Mr. Albert Frank for their critical review of the manuscript.

This research was funded under an Environmental Protection Agency traineeship and Atmospheric Sciences Section, National Science Foundation Grant GA-37571. Funds for data analysis were also provided by the Oregon State University Computer Center.

TABLE OF CONTENTS

LIST OF FIGURES

LIST OF TABLES

A STATISTICAL STUDY OF THE CORRELATION BETWEEN THE SURFACE AND SURFACE GEOSTROPHIC WINDS IN THE WILLAMETTE VALLEY

I. INTRODUCTION

The complex interplay between topography and the synoptic-scale pressure gradient as they effect the wind may be clearly seen in the Willamette Valley of western Oregon. The purpose of this study is to examine the relationship among the surface wind, the horizontal pressure gradient and topography. Such a study has not only scientific merit but also possible practical value since the Willamette Valley has one of the highest air pollution potentials of any area in the United States (Holzworth, 1972). The surface winds in the roughly north-south Willamette Valley are most often northerly in summer and southerly in winter partially due to the channeling effects of the Cascade and Coast Ranges (Olsson et al., 1971). Diurnal surface temperature variations can result in both significant slope winds along the margins of the valley and valley winds in the center. In general, local topography steers the gradient influenced surface flow. However, during periods of stagnation the surface winds often appear to be channeled by topography as surface flow becomes decoupled from flow aloft.

Similar wind patterns have been observed in other valleys. In the Central Valley of California topography and the land-sea effect

seem most influential in July (Frenzel, 1962). For the northern section of this northwest-southeast oriented valley the greatest variation in east-west winds is near Sacramento where the valley is widest. Winds with northerly components are reported only at the northernmost stations. At the southern end the winds generally have easterly or southerly components for at least a portion of the day. Westerly flow entering the valley through the breaks in the Coast Range is diverted north and south parallel to the valley. Diurnal circulations are then superimposed upon this basic flow.

During the night the Kananaskis Valley in southwestern Alberta, Canada (MacHattie, 1968) experiences down-valley winds and within several hours after sunrise insolation causes an increase in up-valley winds. Stronger surface heating then dissipates the local up-valley flow as the result of convective mixing of gradient momentum downward. Hewson (1964) has discussed these types of local diurnal flows, as well as seasonal flows and the impact of local circulations on the transport of pollutants.

Little is known about the response of the surface winds to synoptic-scale pressure fluctuations and the transport of momentum into the valley. In order to gain insight into this problem, this study will investigate diurnal and seasonal variations in the following:

1. The magnitude and direction of the surface winds.
2. The magnitude and direction of the surface geostrophic winds.
3. The relationships between the surface winds and surface geostrophic winds in the Willamette Valley.

II. WIND AND PRESSURE RELATIONSHIPS

Since little is known about the behavior of the surface winds in a valley, a review of the simpler case of the wind and pressure gradient relationship over flat terrain may be a useful first step toward understanding the more complex valley problem.

As a means of comparing the surface wind with that predicted by the pressure gradient, a quantity, R, is defined as the ratio of the magnitudes of the surface wind, V_o, to the surface geostrophic wind, V_{go}. The angle between these winds, α_o, is positive when the surface wind is to the left of the surface geostrophic wind.

A theoretical relationship between V_o, V_g and α_o for a barotrophic atmosphere has been derived by Taylor (1916) and modified slightly by Haltiner and Martin (1957). At the surface of the earth, the wind may be expressed as:

$$V_o = V_g(\cos \alpha_o - \sin \alpha_o) \tag{1}$$

where V_g is the geostrophic wind. This equation predicts that when $\alpha_o = 45°$, the surface wind speed will equal zero. For $V_o > 0$, α_o will be less than 45° and will decrease as R increases. In this study, Equation 1 is modified into the following:

$$V_o = V_{go}(\cos \alpha_o - \sin \alpha_o) \tag{2}$$

which is equivalent to Equation 1 because in a barotrophic atmosphere the geostrophic wind is constant with height. The data indicate that in the Willamette Valley R and α_o are usually negatively correlated. However, results from this study show that the mean α_o is greater than 45° which is thought to be mainly due to terrain effects.

If the height of the boundary layer, h, and the surface roughness length, z_o, are known, a surface-layer α may be calculated (Melgarejo and Deardorff, 1974) as:

$$\sin \alpha = -a\{[\ln(h/z_o)-b]^2+a^2\}^{-1/2} \text{ sign } f \qquad (3)$$

where f is the Coriolis parameter, a and b are stability functions for momentum which are expected to be dependent on the ratio of h and the Monin-Obukhov length, L. Because vertical sounding data are not utilized in this study, a layer mean α cannot be calculated and only general comparisons can be made between the Willamette Valley and the baroclinic cases referenced here.

For baroclinic conditions, the manner in which the vertical momentum transport alters the stress profile is dependent on the relationship of the magnitude and direction of both the thermal wind in the planetary boundary layer and the surface geostrophic wind (Hoxit, 1974). In a theoretical study, Thompson (1974) used the slab method to investigate the relationship between the thermal wind and

surface isobars. His conclusions are similar to observations (Bernstein, 1973) of flow above an ocean which show that maximum α_o values occur with cold air advection because the layer in which advection is occurring is most unstable.

Hasse (1974) states that for flow above the ocean α is least (10°) with near-neutral stability. For stable and unstable cases deviations are generally 20° or greater. For a given stability regime, the relationship between the winds above the ocean and the geostrophic winds is fairly linear at low wind speeds. For example:

$$V_o = aV_g + b \tag{4}$$

where V_o is the surface wind speed, V_g is the geostrophic wind speed and a and b are both stability dependent constants. Hasse states that when the magnitude of the geostrophic wind is greater than 25 m sec^{-1} the average surface winds are smaller than that calculated from Equation 4. In this study an attempt is made to calculate a second order equation which statistically relates the wind in the Willamette Valley to the magnitude of the surface geostrophic wind. With a weak pressure gradient the surface wind speed frequently exceeds the geostrophic wind speed and α is variable. At this time accelerations may be important and wind directions difficult to measure accurately. In the Willamette Valley, both R and α_o are independently so strongly influenced by terrain that it is difficult to

determine their exact interrelationship statistically. They will be shown to be negatively correlated.

In the slightly more complex case of flow above a gently rolling countryside, small stability differences in near-neutral cases have a significant effect on R (Deacon, 1973). Slight instability results in much larger R values and smaller α_o values than slightly stable conditions (Appendix I). In the Willamette Valley the largest average R values are observed during periods of instability. Because of terrain influences α_o is not simply related to stability, as is evident from the data analyses of this study.

III. SITE DESCRIPTION AND VALLEY CLIMATOLOGY

The 200 km long Willamette Valley runs north from Eugene (110 m msl) where its average width is 30 km to Salem (60 m msl), the location around which this study is centered. It then bends north-northeastward and widens to 60 km. Portland (7 m msl) is located at the end of the valley at the confluence of the Willamette and Columbia Rivers (Figure 1). Hewson (1972) stated that the Willamette Valley can be likened to a large box with several windows and doors. The Cascade Range forms a solid east wall roughly 2 km high. To the west the Coast Range is a lower barrier ranging 0.5 to 1 km high containing three "windows"; namely, the Florence Corridor northwest of Eugene, the Yaquina and Alsea Corridors west of Corvallis and the Van Duzer Corridor north-northwest of Salem. Marine air penetration through these three gaps has a significant effect on the weather along the western edge of the valley. The "doors" in the box are located at the intersection of the Willamette Valley and the Columbia Gorge and the lid is determined by the upper limit of the mixing height.

The valley is annually subjected to two major pressure regimes. In winter the persistence of low pressure off the coast supports southerly flow moving down the valley. In summer the northward extension of the subtropical anticyclone supports northerly flow moving up the valley. The anticyclone also pushes surface water seaward

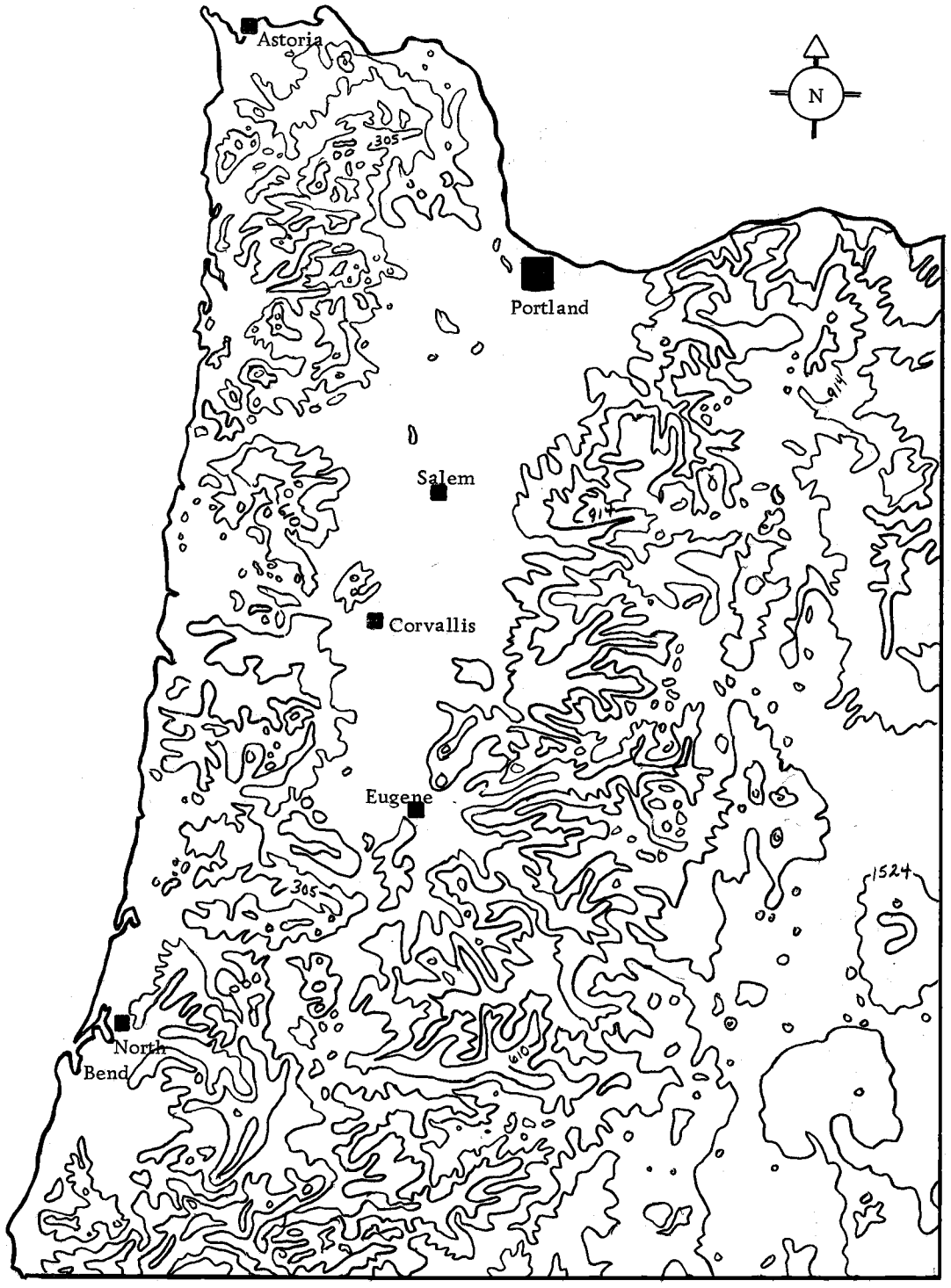

Figure 1. Map of the Willamette Valley and western Oregon (after Aeronautical Chart and Information Center, 1970).

allowing the upwelling of cold water in a 10 km wide zone. A shallow layer of cool air is produced over these coastal waters while at the same time a thermal trough prevails over western Oregon frequently extending northward into the Willamette Valley. According to Cramer and Lynott (1961) when this occurs the pressure may be as much as 6 mb higher along the coast than in the Willamette Valley (80 km distant). These conditions frequently result in marine air penetration through the Coast Range into the valley by late afternoon. The depth of the marine air layer is usually less than 900 m. However, this type of cross-valley flow is exceptional as indicated by the predominant occurrence of surface winds parallel to the valley at Salem (Figure 2).

Although considerable variation in wind direction exists throughout the year, the spring and fall months experience the greatest variation as would be expected since they are transitional seasons.

Diurnal as well as seasonal changes are important. The Salem winds at 0600[1] are most frequently from the south-southwest (Figure 3). This is attributable to the increased stability resulting from diurnal cooling and perhaps nocturnal drainage of colder air into the valley. Wintertime southerly winds then become increasingly westerly by 1600 before shifting to a more southerly direction by 2000. In the

[1] All times are Pacific Standard Time.

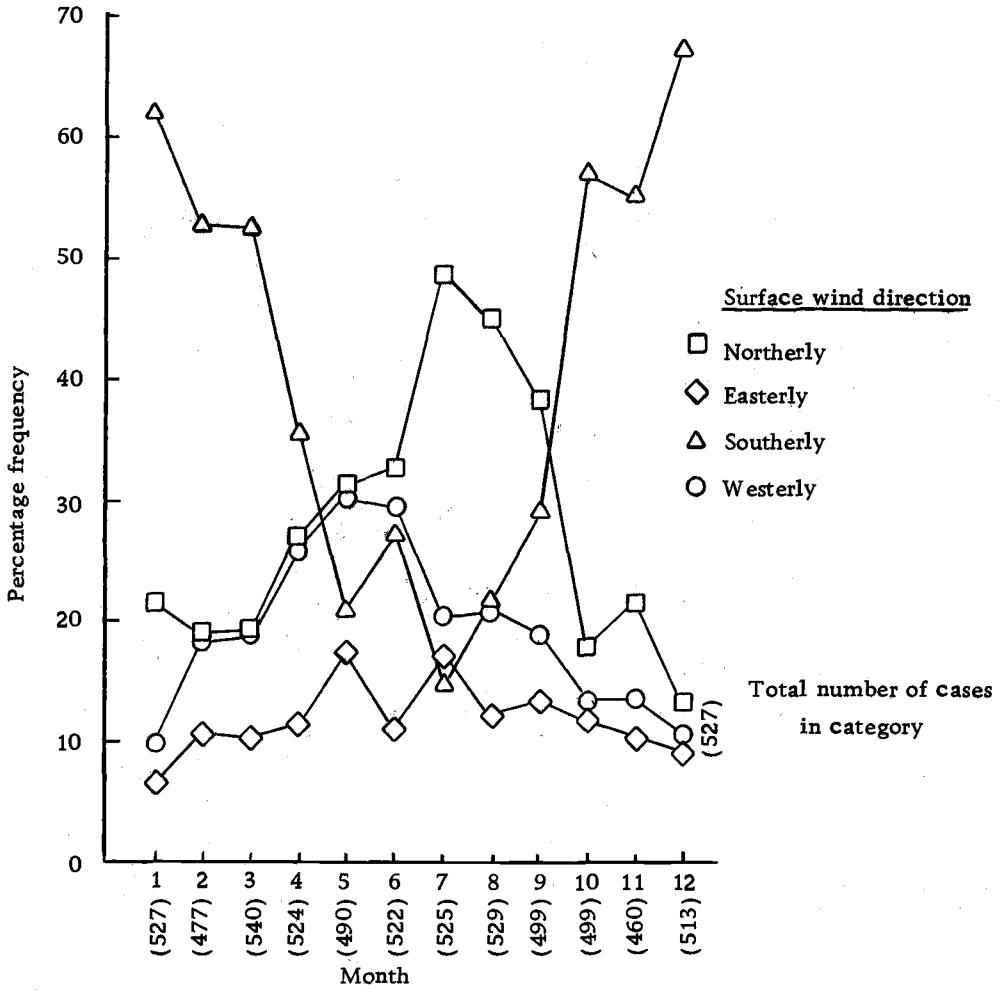

Figure 2. Monthly surface wind direction frequency.

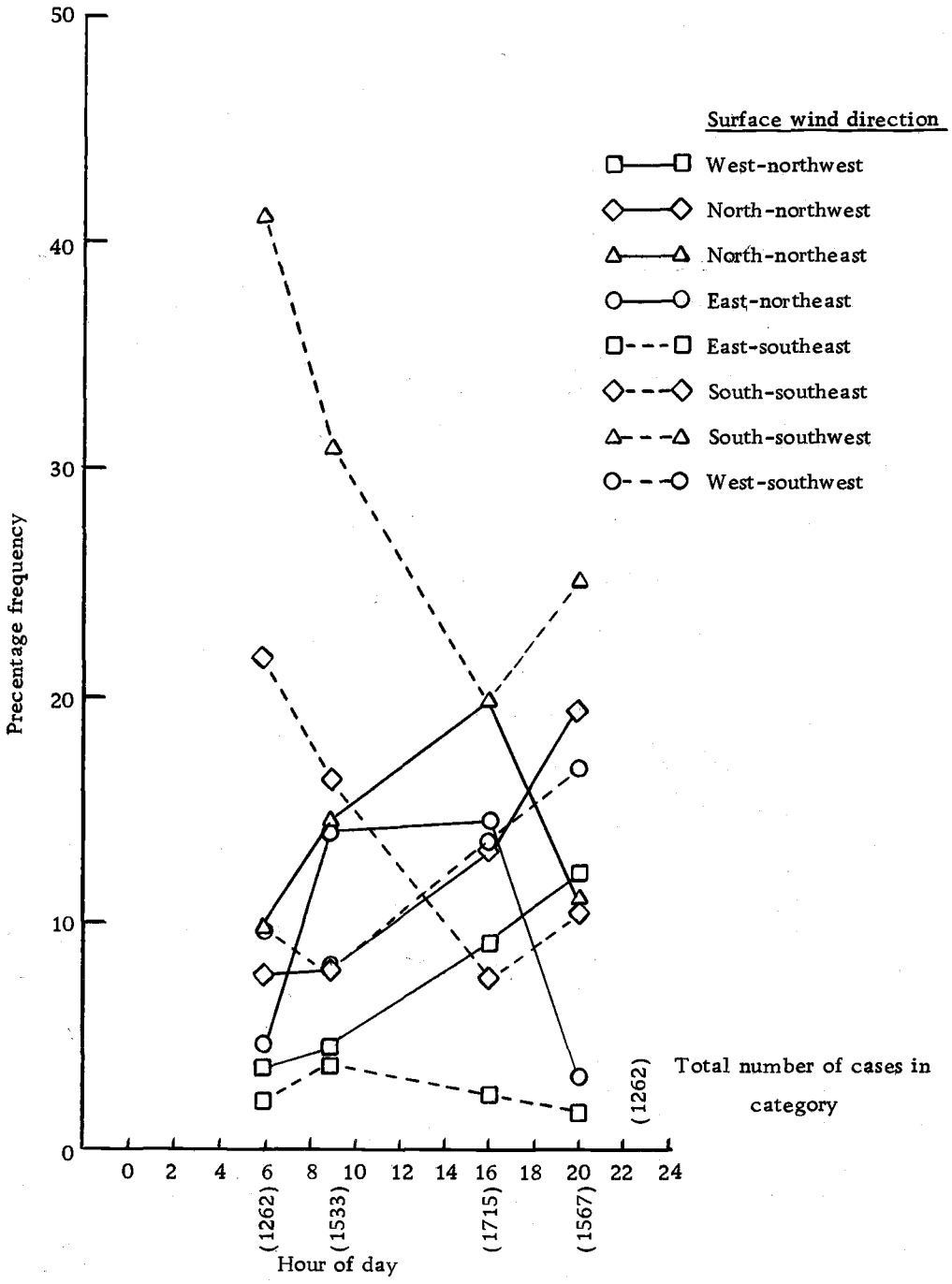

Figure 3. Hourly frequency of surface wind direction.

summer the number of northerly flow cases reported increases throughout the morning and afternoon. By 2000 north-northwest winds are most frequent, presumably due to marine air penetration.

Speed variations are also of interest in understanding mass and pollution transport. Diurnal wind speed variations are shown in Figure 4. Wind speed varies from an average of 3 m sec^{-1} in the morning to 4.5 m sec^{-1} in mid-afternoon when thermodynamic stability is at a minimum. Greatest speeds occur with southerly winds (Figure 5). Wind speed is largest in the winter months, 4 m sec^{-1} and it decreases slightly to 3.4 m sec^{-1} in the summer months (Figure 6).

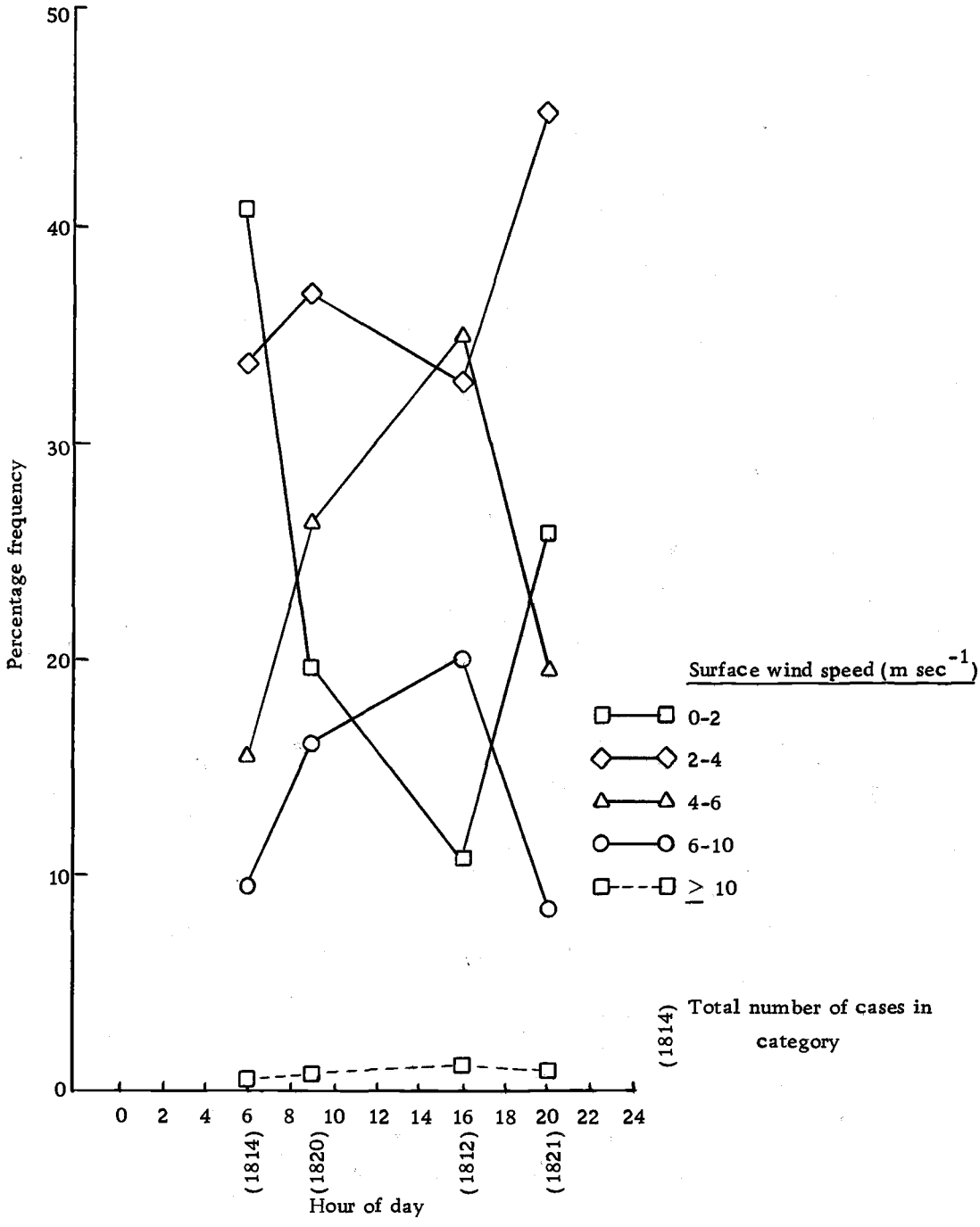

Figure 4. Hourly surface wind speed frequency.

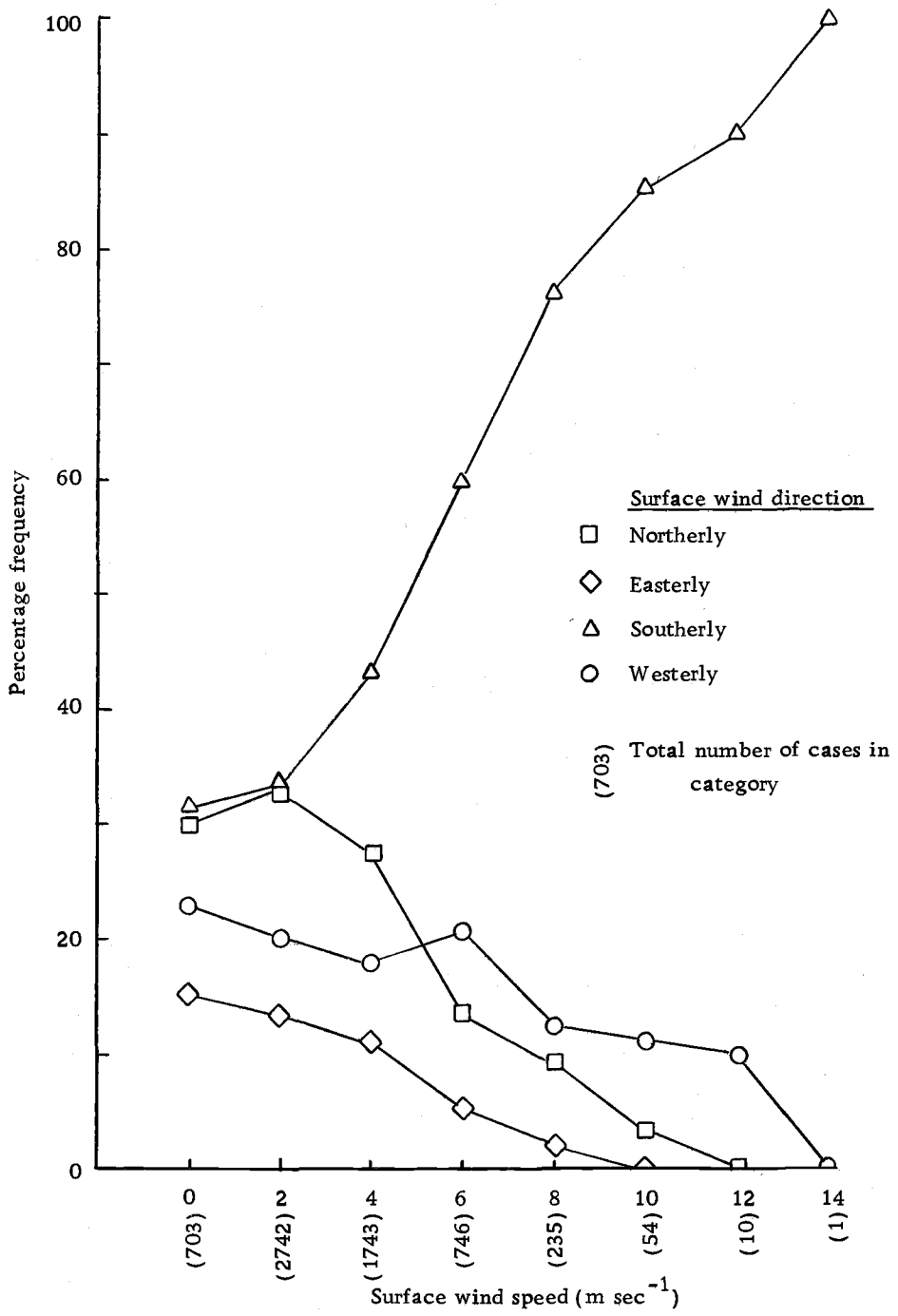

Figure 5. Surface wind direction frequency for selected surface wind speed categories.

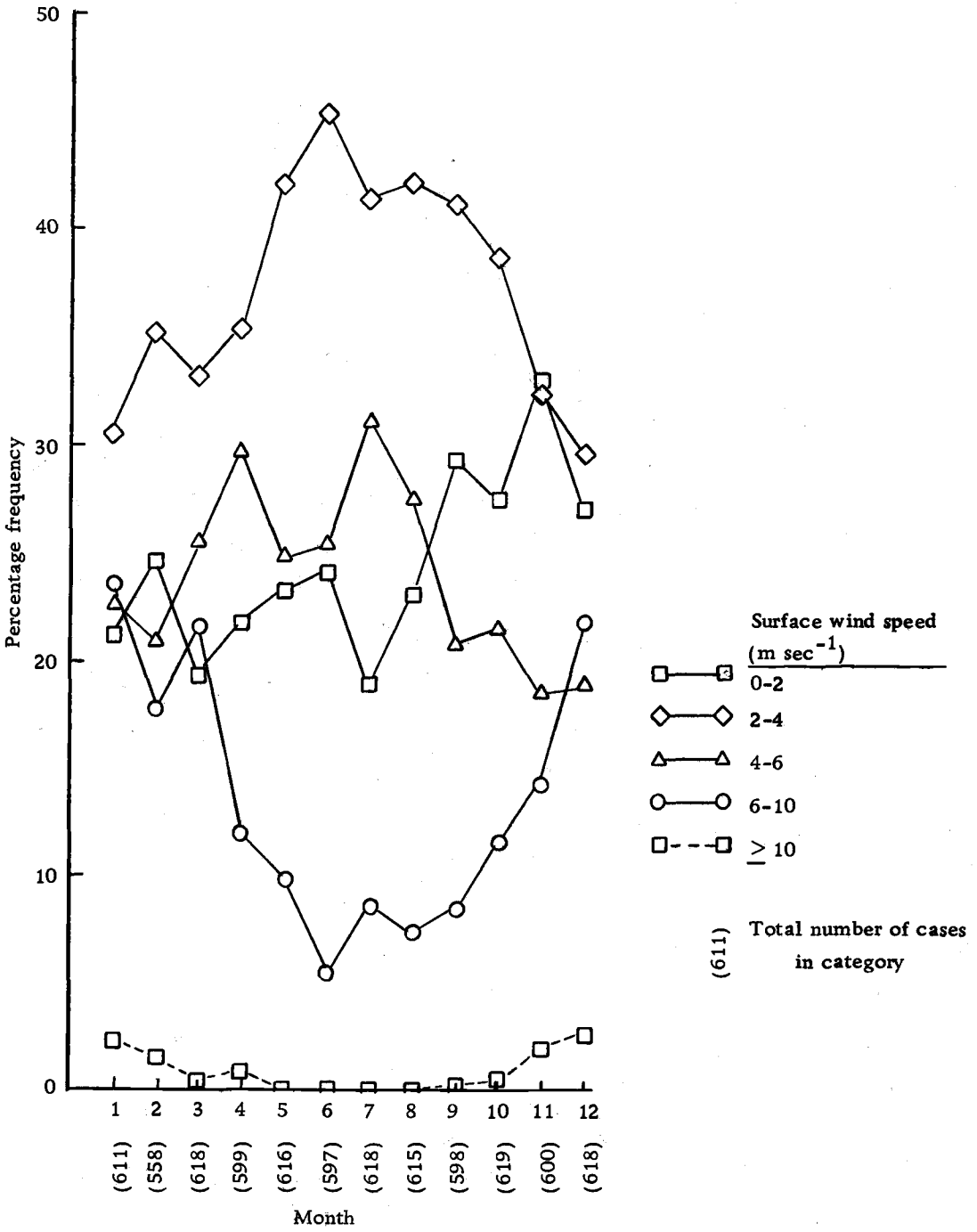

Figure 6. Monthly frequency of surface wind speed.

IV. DATA DESCRIPTION AND REDUCTION METHODS

National Weather Service observations for 1953 through 1957 were obtained on magnetic tape from Ashville Climatic Center in Ashville, North Carolina for Eugene, Salem and Portland. In addition, data were obtained for Astoria, at the mouth of the Columbia River, and for North Bend 300 km south (Figure 1). These are the coastal stations used in this study to help estimate the east-west pressure gradient.

In order to reduce the amount of data and computer time, representative hours of 0600, 0900, 1600 and 2000 were selected. The 0600 observation is assumed to typify nocturnal meteorological conditions. By 0900 surface heating has usually destroyed or is in the process of destroying any residual nighttime inversion. By 1600 maximum insolation has resulted in the greatest amount of turbulent mixing. Atmospheric stability is rebuilding by 2000 and in summer, on those days which it occurs, marine air penetration is fully developed at this time.

For the purposes of this study the seasons in western Oregon are defined as follows:

winter	November through February
winter core	December and January
summer	June through September
summer core	July and August
transitional	March, April, May, October

This categorization is based on climatic normals of cloud cover and precipitation. Winter and summer core months are compared with their respective seasons to contrast periods of most intense seasonal pressure patterns with pressure developments.

In this study, the relationship between the winds at Salem and the pressure gradient are estimated by using the pressure at surrounding stations. The surface geostrophic flow is defined to be:

$$u_{go} = -\frac{1}{\rho f}\frac{\partial p}{\partial y} \tag{5}$$

$$v_{go} = \frac{1}{\rho f}\frac{\partial p}{\partial x} \tag{6}$$

where u_{go} and v_{go} are the x and y components of the surface geostrophic wind, ρ, the density of air, is assumed constant at approximately 1.2×10^{-3} kg m^{-3}, the Coriolis parameter, f, is 10^{-4} sec^{-1} at 45° north latitude and p is the mean pressure. The following finite difference forms will be used to approximate the pressure gradients:

$$\frac{\partial p}{\partial x} \approx \frac{\Delta p}{\Delta x} = \frac{P_{SLE} - P_{PNT}}{X_{SLE} - X_{PNT}} \tag{7}$$

$$\frac{\partial p}{\partial y} \approx \frac{\Delta p}{\Delta y} = \frac{P_{PDX} - P_{EUG}}{Y_{PDX} - Y_{EUG}} \tag{8}$$

where $P_{PNT} = (P_{AST}+P_{OTH})/2$, P_{PDX}, P_{EUG}, P_{SLE}, P_{AST} and P_{OTH} are the pressures at Portland, Eugene, Salem, Astoria and North Bend, respectively and $X_{(\ )} - X_{(\ )}$ and $Y_{(\ )} - Y_{(\ )}$ are the distances separating the two stations referenced in the parentheses.

Thus, the north-south component of the pressure gradient at Salem, $\partial p/\partial y$, is estimated by calculating the pressure difference between Portland and Eugene divided by the distance separating the two stations. For the east-west component of the pressure gradient, p is estimated first from a point on the coast midway between Astoria and North Bend by averaging the pressure between these two stations. This pressure is then subtracted from that at Salem and divided by the distance between the two points. Unavoidably this gradient is not centered about Salem. The north-south component estimate is centered 17 km southeast and the east-west component estimate is centered 40 km west-southwest of Salem. Stations in central Oregon are not used to calculate east-west component gradients because the relationship between circulations in the valley and east of the Cascade Range is not clearly understood and flows are possibly not strongly coupled. Furthermore, pressure cannot be accurately reduced to sea level.

The magnitude of the surface geostrophic wind may be expressed as $\sqrt{u_{go}^2 + v_{go}^2}$. The direction of the surface geostrophic wind is simply the arctangent of the quotient of v_{go}/u_{go}. The ratio of the

surface wind to the surface geostrophic wind is R, while the difference between the direction of the surface geostrophic wind and the surface wind is defined to be α_o. For ease in data reduction, each observation of α_o greater than 180° is changed to the negative angle (e.g., $\alpha_o = 270°$ is converted to $\alpha_o = -90°$). With this notation α_o is positive if the surface wind has a component directed toward low pressure to the left of the surface geostrophic wind. For surface winds less than 1.55 m sec^{-1} α_o is not calculated since wind speed and direction are reported as calm.

V. ANALYSIS OF THE DATA

Only 0.5% of the data were lost as a result of missing or inaccurate reports. In an additional 15% of the observations, winds of less than 3 kt were reported at Salem so that α_o is not calculated for these cases.

The Wintertime Flow Situation

The wintertime surface geostrophic flow is most often southerly (Figure 7). With this surface geostrophic wind direction, α_o equals 20° (Figure 8). Westerly surface geostrophic winds occur with the second greatest frequency and with moderate surface winds (greater than 10 m sec^{-1}) α_o assumes a value of 80° (Figure 9). As a result of averaging all of the observations, α_o is most often 60° (Figure 10). In other words, the average surface winds are usually parallel to the valley regardless of the orientation of the pressure gradient which accounts for the strong variation of α_o.

The average magnitude of the surface geostrophic wind is stronger in winter than in summer (Table 1) and is strongest when the surface geostrophic wind is parallel to the valley because gradient momentum then has a longer distance over which to mix downward to the surface. Not surprisingly, the core months in both winter and summer experience stronger surface geostrophic winds than either

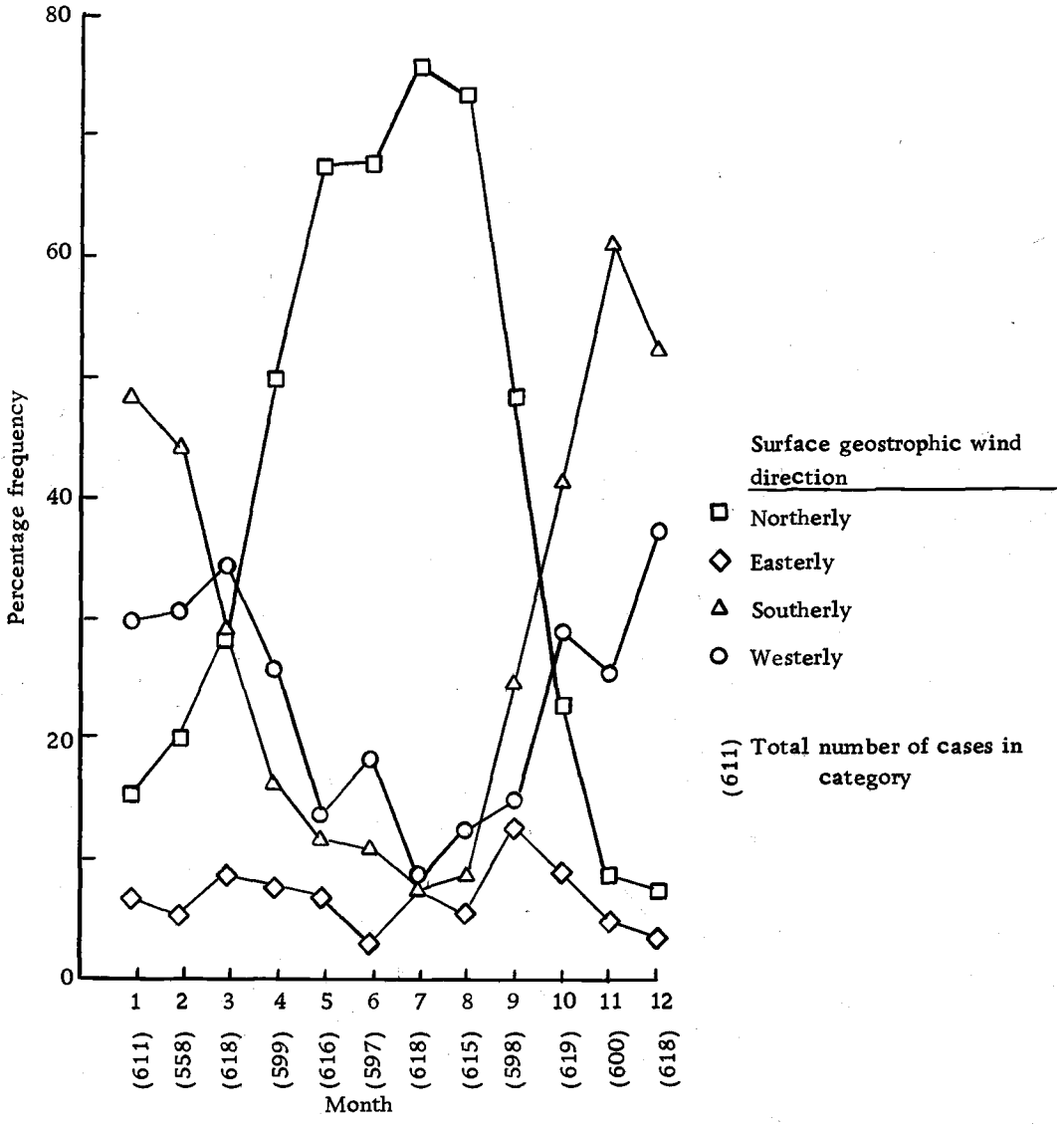

Figure 7. Monthly frequency of surface geostrophic wind direction.

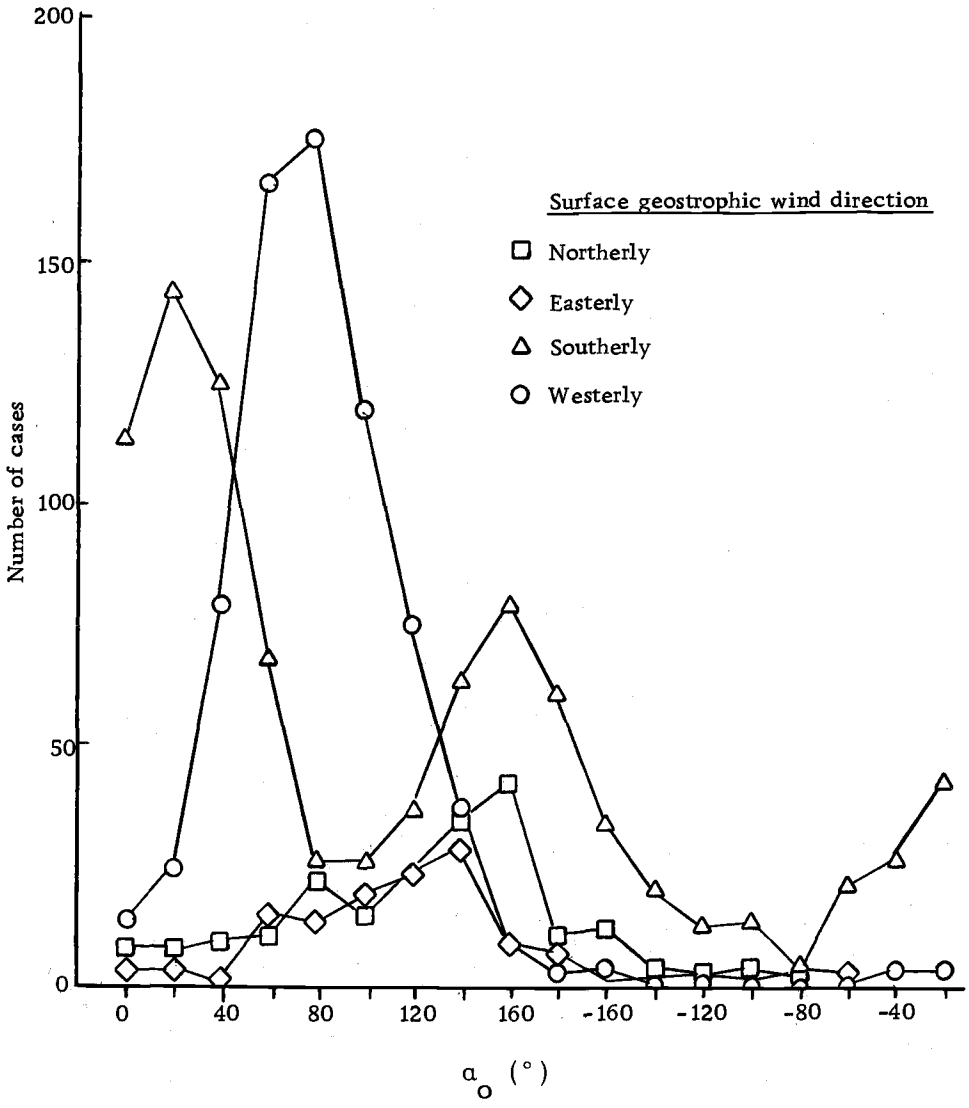

Figure 8. Surface geostrophic wind direction frequency for selected a_o categories (winter only).

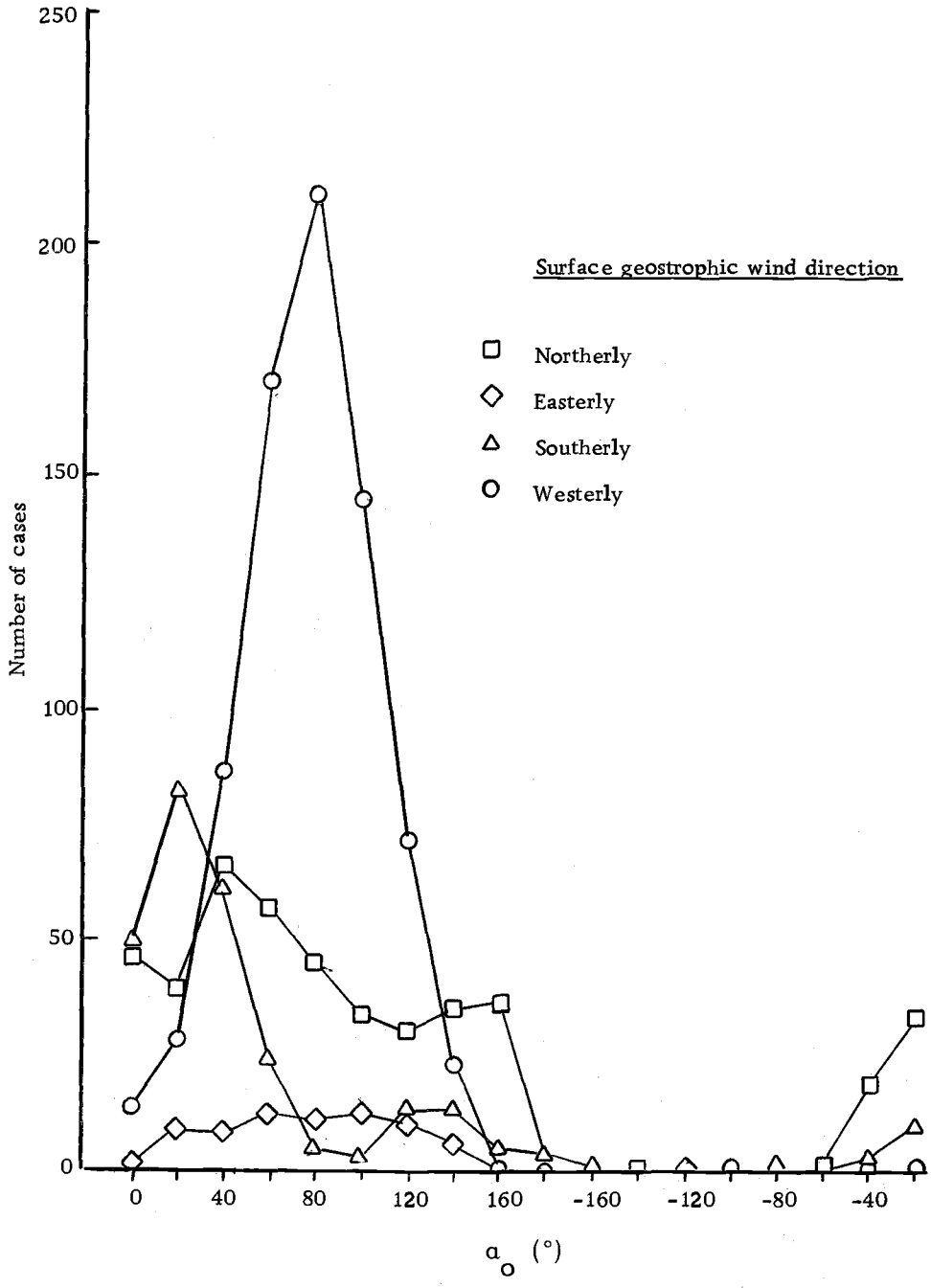

Figure 9. Surface geostrophic wind frequency for selected α_o categories (moderate and large surface winds).

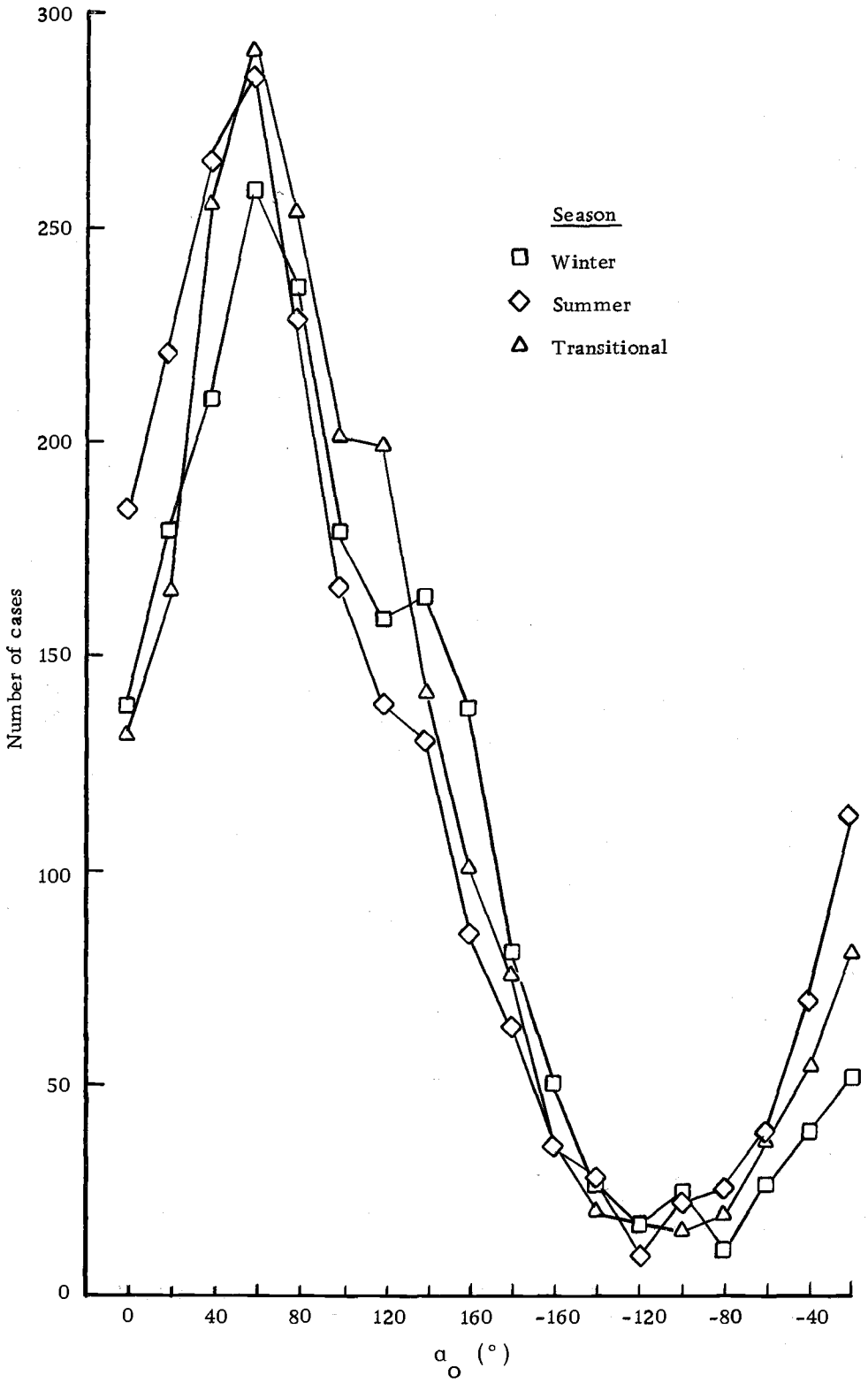

Figure 10. Seasonal α_o frequency.

respective season as a whole or the transitional seasons (Figure 11). In winter perhaps this is related to the sharp pressure gradient caused by off-shore cyclone occurrence. Although winter winds are stronger than summer winds, R is less since wintertime pressure gradients are larger (Table 1); that is thermodynamic stability decreases the winter wind relative to the surface geostrophic wind speed.

Table 1. Mean values of surface wind speed, geomag and R.

	Winter	Summer	Winter Core	Summer Core
Surface wind ($m\ sec^{-1}$)	4.0	3.4	4.2	3.6
Geomag ($m\ sec^{-1}$)	14.2	12.5	15.6	13.8
R	0.37	0.46	0.36	0.46

A regression equation is calculated to relate the pressure gradient to the surface winds. It is intended that this equation might be operationally useful. This relationship for all winter observations is as follows:

$$\text{wind speed} = 0.66G - 0.02G^2 \tag{9}$$

where

$$G = \sqrt{43.18(P_{PDX}-P_{EUG})^2 + 190.84(P_{SLE}-P_{PNT})^2} \tag{10}$$

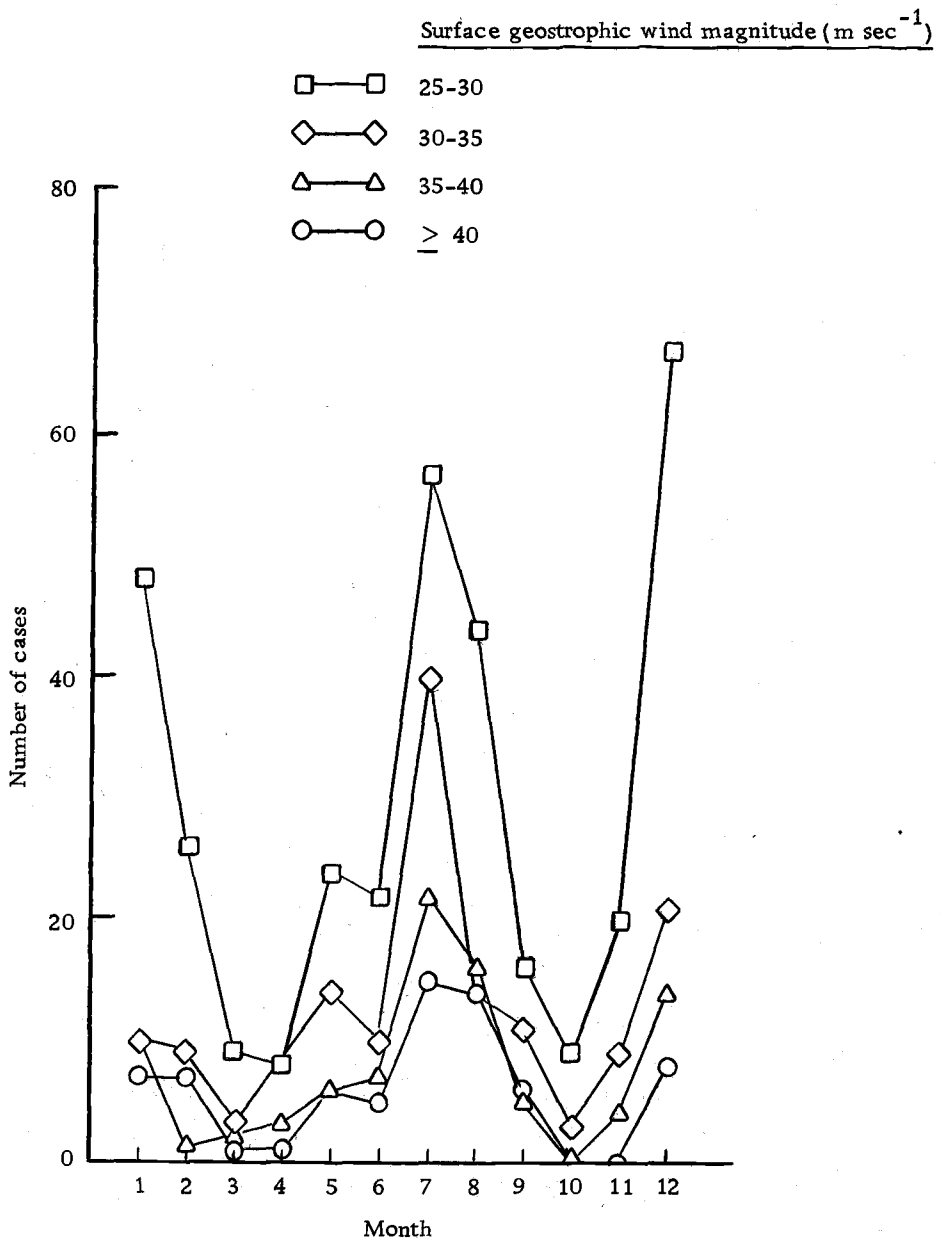

Figure 11. Monthly large geostrophic wind speed frequency.

and the other symbols are as defined above. Pressure is in millibars and the surface wind speed is in m sec^{-1}. The results of the F-test show that this equation has low statistical significance, but takes into account the east-west pressure component, unlike some regression equations presently used in forecasting.

Figures 12 through 14 demonstrate the diurnal dependence of the meteorological parameters. In winter the direction and magnitude (Figure 12) of the surface geostrophic wind exhibit little diurnal variation. Average winter R also varies little (Figure 13) with only a weak afternoon maximum, reflecting small daily fluctuations in stability. With weak winter heating, pressure gradients are primarily related to cyclone occurrence which statistically appears to be relatively independent of time of day.

Figure 14 shows that little diurnal change occurs in the wintertime relationship between the magnitude of the surface geostrophic wind and R. This is due to stability. The linear correlation between the surface geostrophic wind speed and R is negative for all hours of the day. This appears to be reasonable since surface stress and therefore surface stress divergence are thought to be proportional to the square of the magnitude of the surface geostrophic wind such that increasing surface geostrophic wind speed implies decreasing R. The data indicate that an increase in the surface geostrophic wind

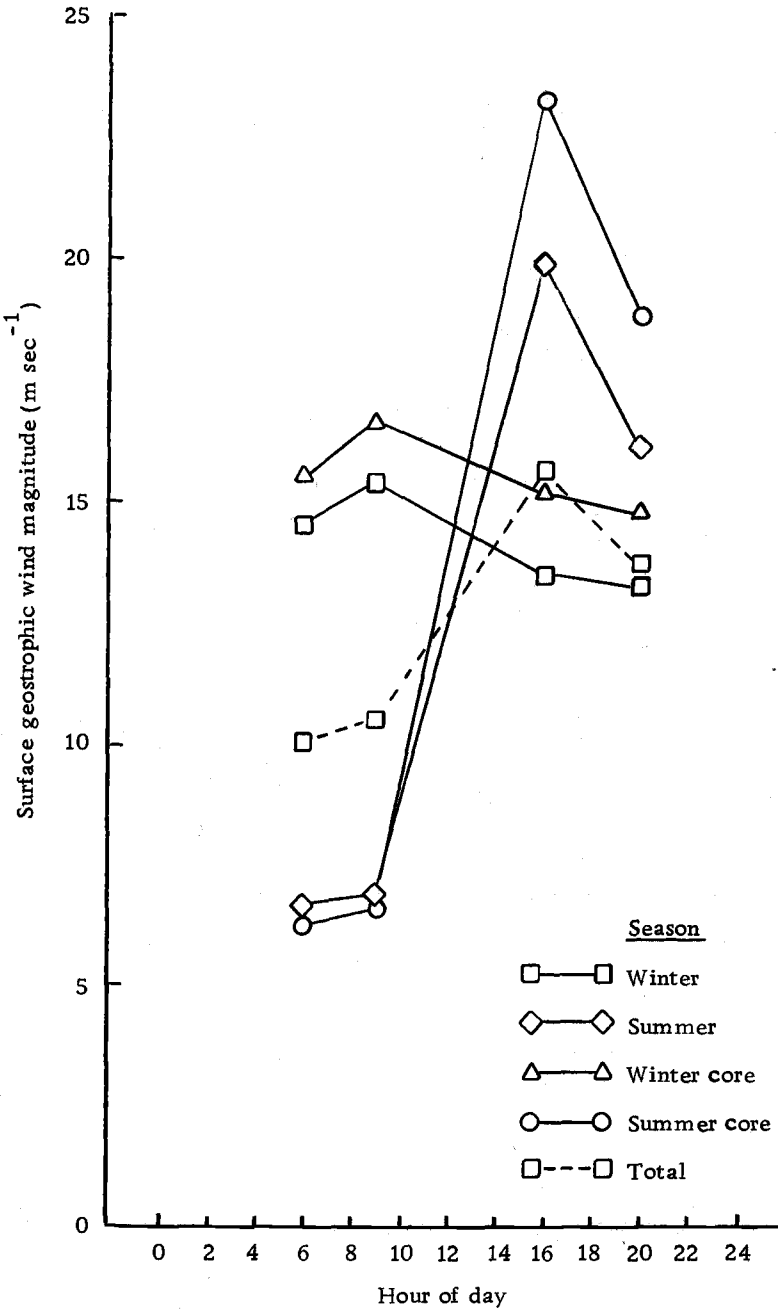

Figure 12. Hourly surface geostrophic wind magnitude (by season).

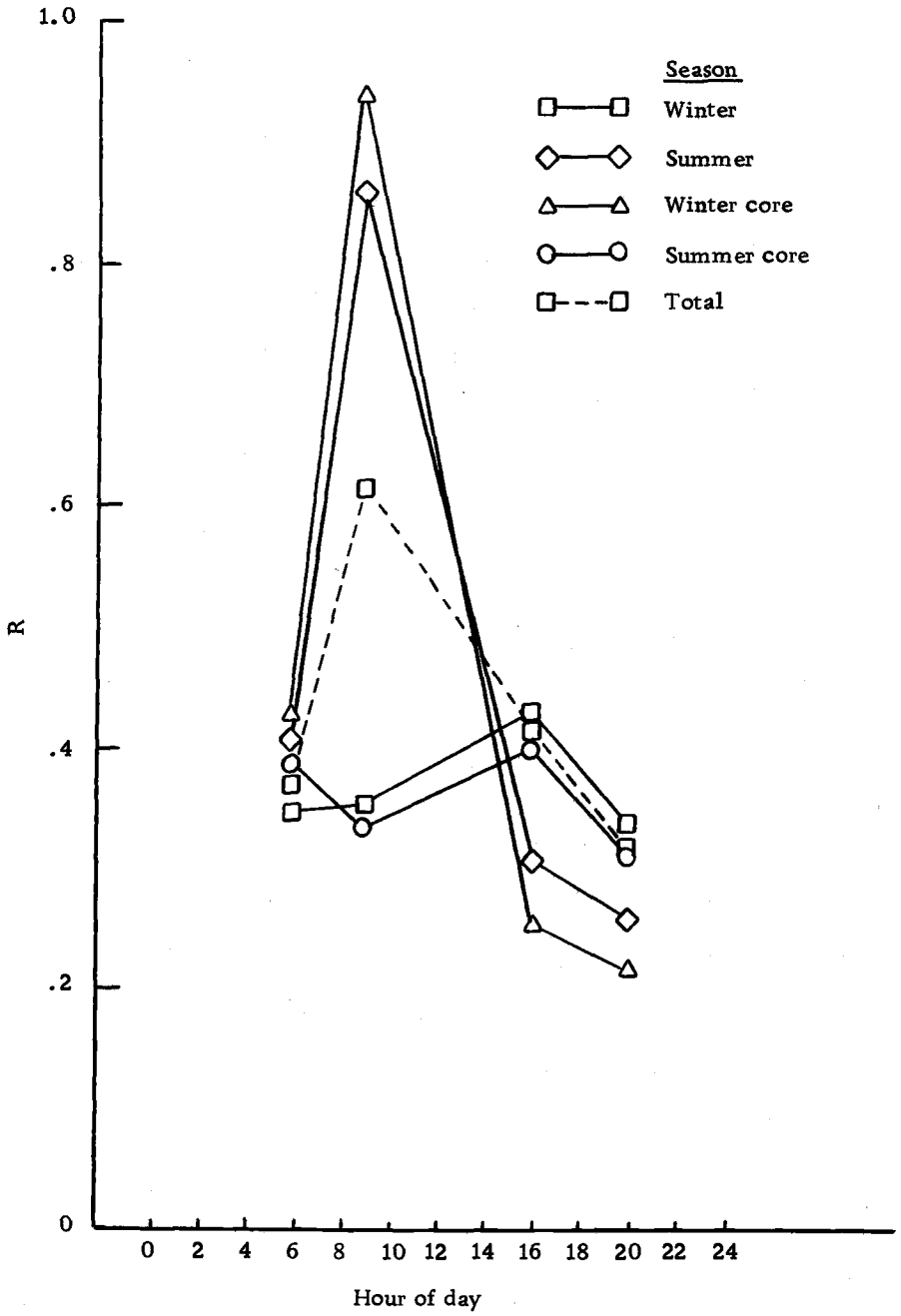

Figure 13. Hourly R (by season).

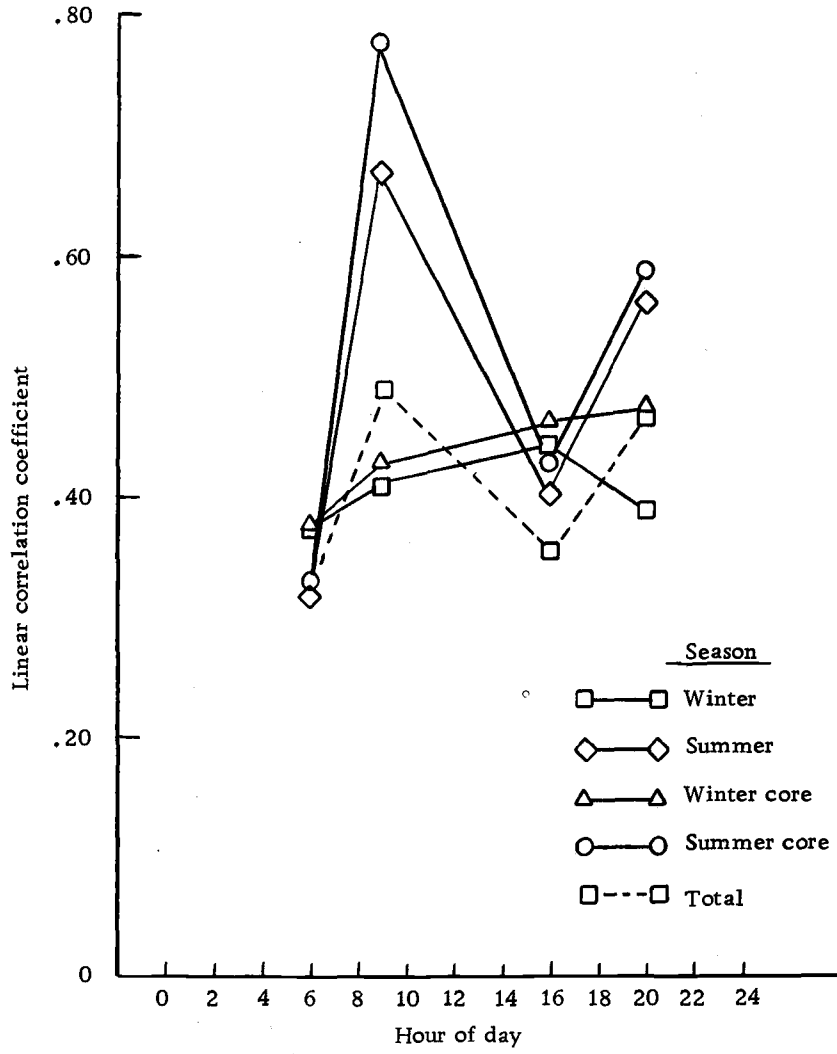

Figure 14. Hourly linear correlation coefficient (for seasonal correlation between surface geostrophic wind speed and R).

speed also suggests greater mixing and a decrease in the variability of α_o.

The Summertime Flow Situation

During the summer, the subtropical anticyclone is extended northward. The average pressure gradient is weaker than in winter causing the average magnitude of the surface geostrophic wind to be about 2 m sec^{-1} less than in summer. Average winds decrease only 0.5 m sec^{-1} so summertime R is 125% greater than in winter. Almost half (43%) of the supergeostrophic wind cases ($R > 1$) occur during the summer months, particularly during July and August. Although the summertime average is less, at certain times the magnitude of the surface geostrophic wind may become large when differential surface heating is most intense. One-third of the observations reporting a large surface geostrophic wind speed (greater than 25 m sec^{-1}) occur during July and 45% during June through August. When the surface geostrophic wind speed is moderate or large (larger than 10 m sec^{-1}) the surface wind is predominantly parallel to the valley regardless of the direction of the surface geostrophic wind. The magnitude of the surface geostrophic wind is largest and most variable when the surface geostrophic wind is northeasterly.

In the summer the surface geostrophic wind is most frequently northeasterly, except in early morning (Figure 15). During the

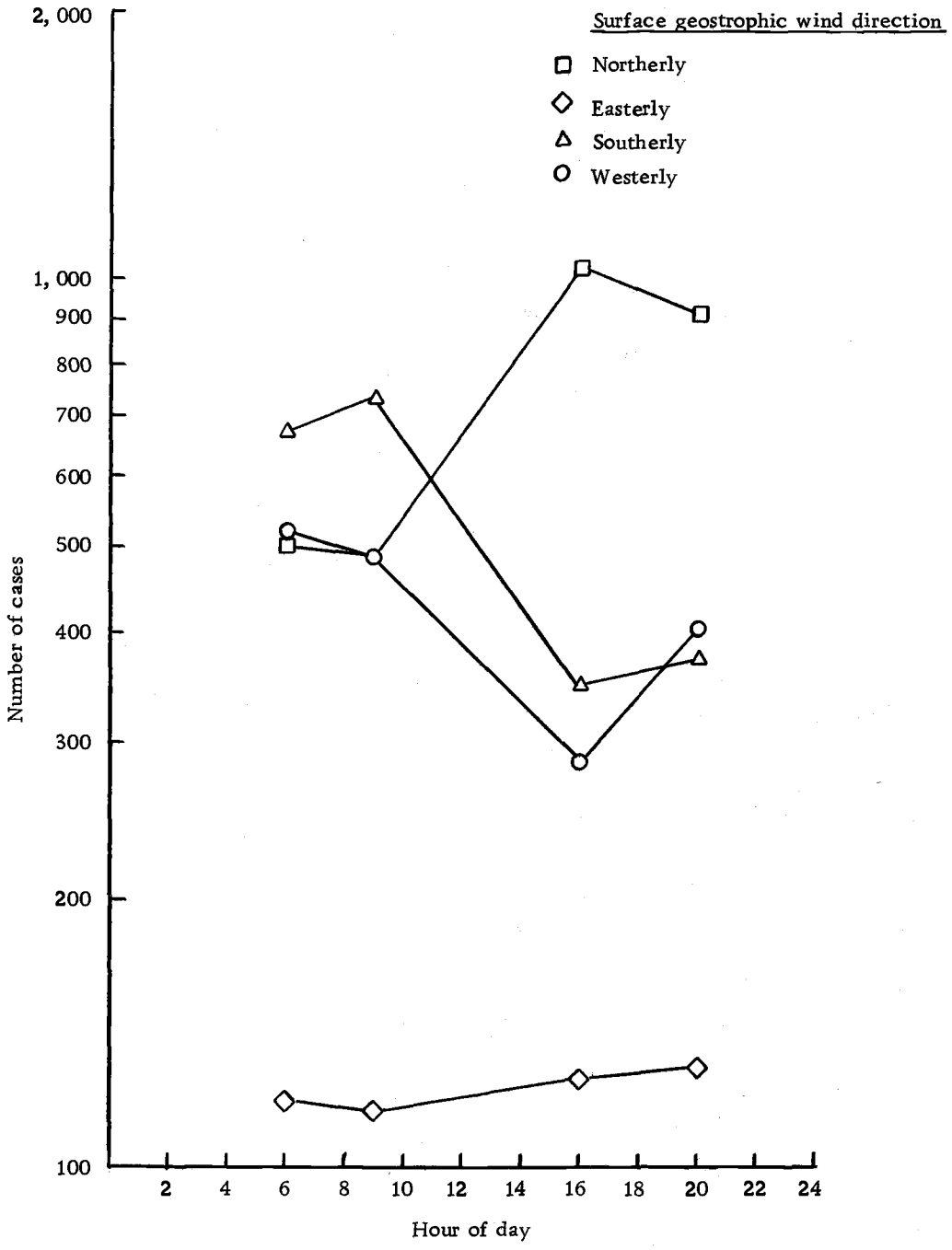

Figure 15. Hourly surface geostrophic wind direction frequency (note log scale).

summer core months the average surface geostrophic wind is more nearly north-northeasterly which may be a result of averaging in the northwesterly marine air flow cases.

With a northerly surface geostrophic wind, α_o is most frequently 60° (Figure 16). The large α_o values may be explained by marine air invasions when flow adjustment to the pressure gradient is not maintained. Although α_o is more variable than in winter, its behavior again suggests a preference for surface winds along the valley. When the surface geostrophic wind is parallel to the valley α_o is most variable. In September α_o exhibits the least variability of the entire year as it assumes a value of 20°.

Diurnal variation of the winds is considerably greater in summer than in winter. The average direction of the surface geostrophic wind rotates counterclockwise with daytime heating and clockwise at night which is in agreement with MacHattie (1968) and the thermodynamics of the valley. Northward extension of the California trough between 0600 and 0900 is evident in the summer. The 1600 and 2000 northwesterly shift in the surface geostrophic wind reflects the effects of strong differential heating.

In spite of the diurnal rotation of the surface geostrophic wind, as in winter, the most frequently observed value of α_o is about 60°. This frequency maximum is most pronounced at 1600 and 2000 (Figure 17). Thus, α_o is usually not within the +10° to +40° predicted

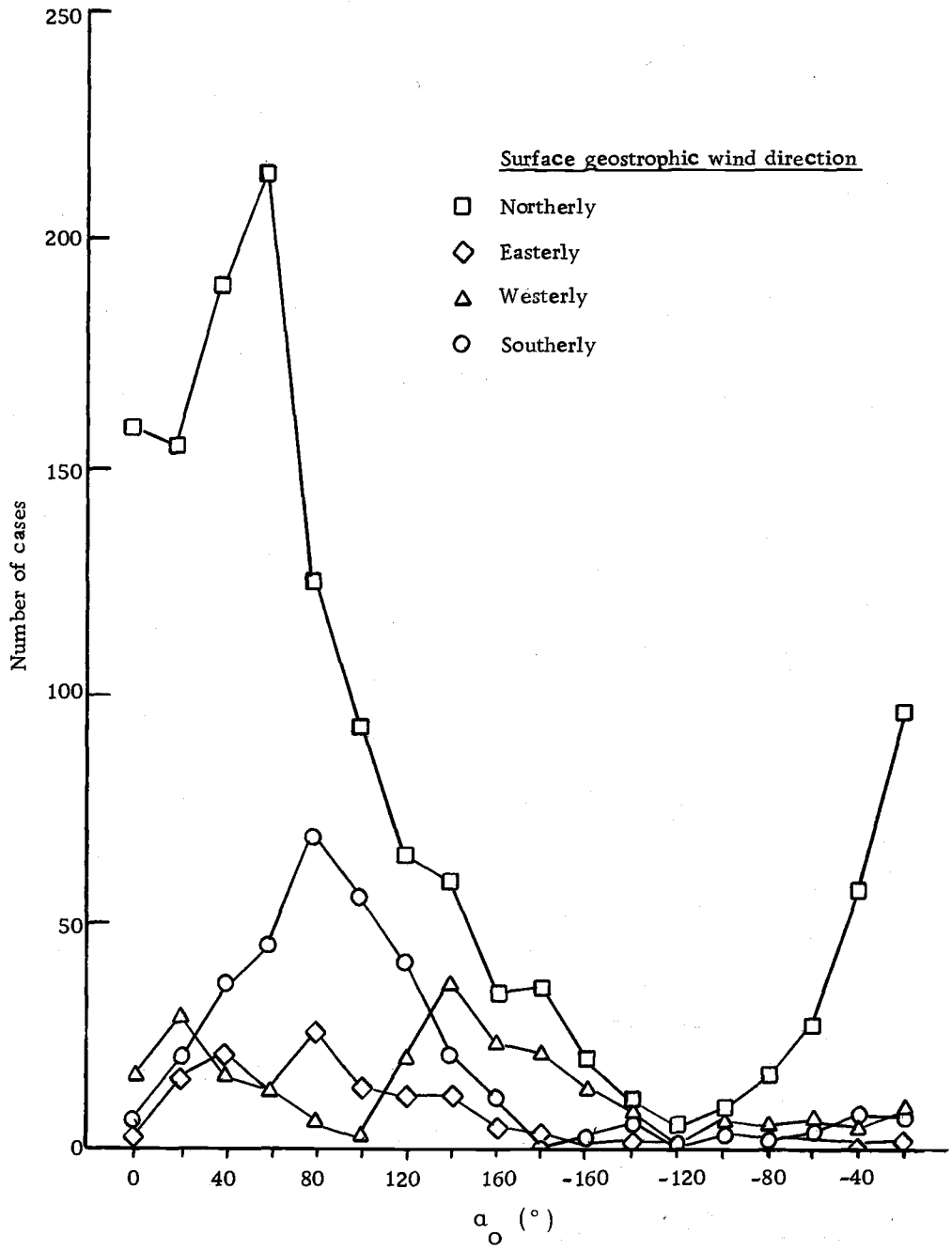

Figure 16. Surface geostrophic wind frequency for selected cases of a_o (summer only).

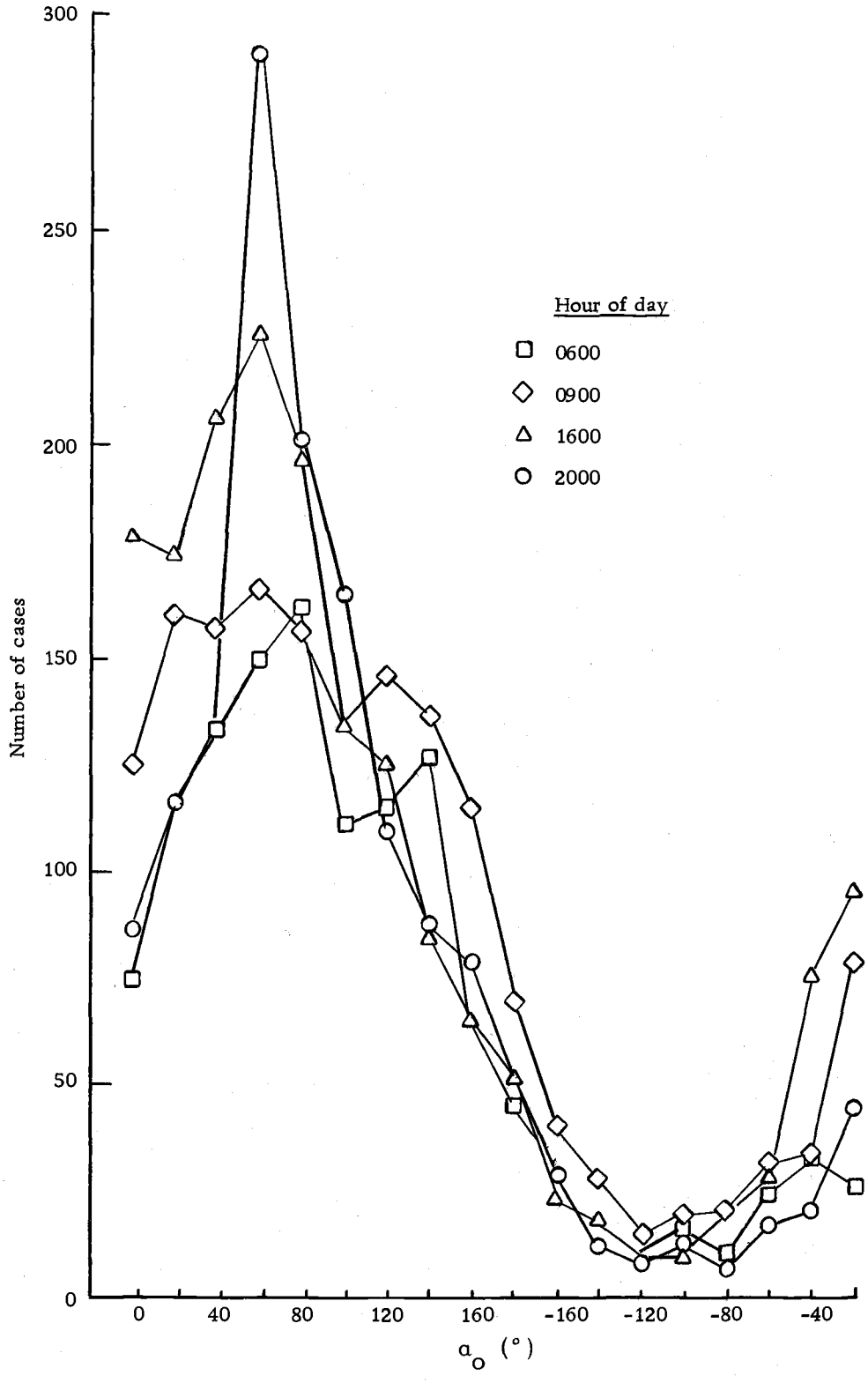

Figure 17. Hourly a_o frequency.

by theory. This departure may be explained by terrain influences, small scale accelerations and computational errors which can result because of the inaccurate measurement of pressure, an asymmetrical grid and unresolved subsynoptic pressure gradients which can be generated by heating on a sloped surface.

At 0900 when α_o is increasingly variable because insolation is destroying nighttime stability, R is at its diurnal maximum. The magnitude of the surface geostrophic wind is still small at this time so relatively light small scale generation of winds and pressure gradients may be important. Such small scale pressure gradients cannot be resolved by a grid as coarse as the one used in this study. The observed relationship between the surface geostrophic wind speed and R is shown in Figure 18. Half of the supergeostrophic wind cases occur at 0900 when the surface geostrophic wind speed is small (Figure 19). The sharp decrease in average R after 0900 reflects the rapid increase in the magnitude of the surface geostrophic wind. The surface wind cannot accelerate rapidly enough in such short time and space scales to maintain a constant R.

The summertime 0900 linear correlation between the surface geostrophic wind speed and R is again negative with the highest value, -0.78 in July and August and a value of -0.67 for June through September. Minimum correlations occur at 0600 when surface flow is decoupled from the synoptic-scale pressure gradient due to

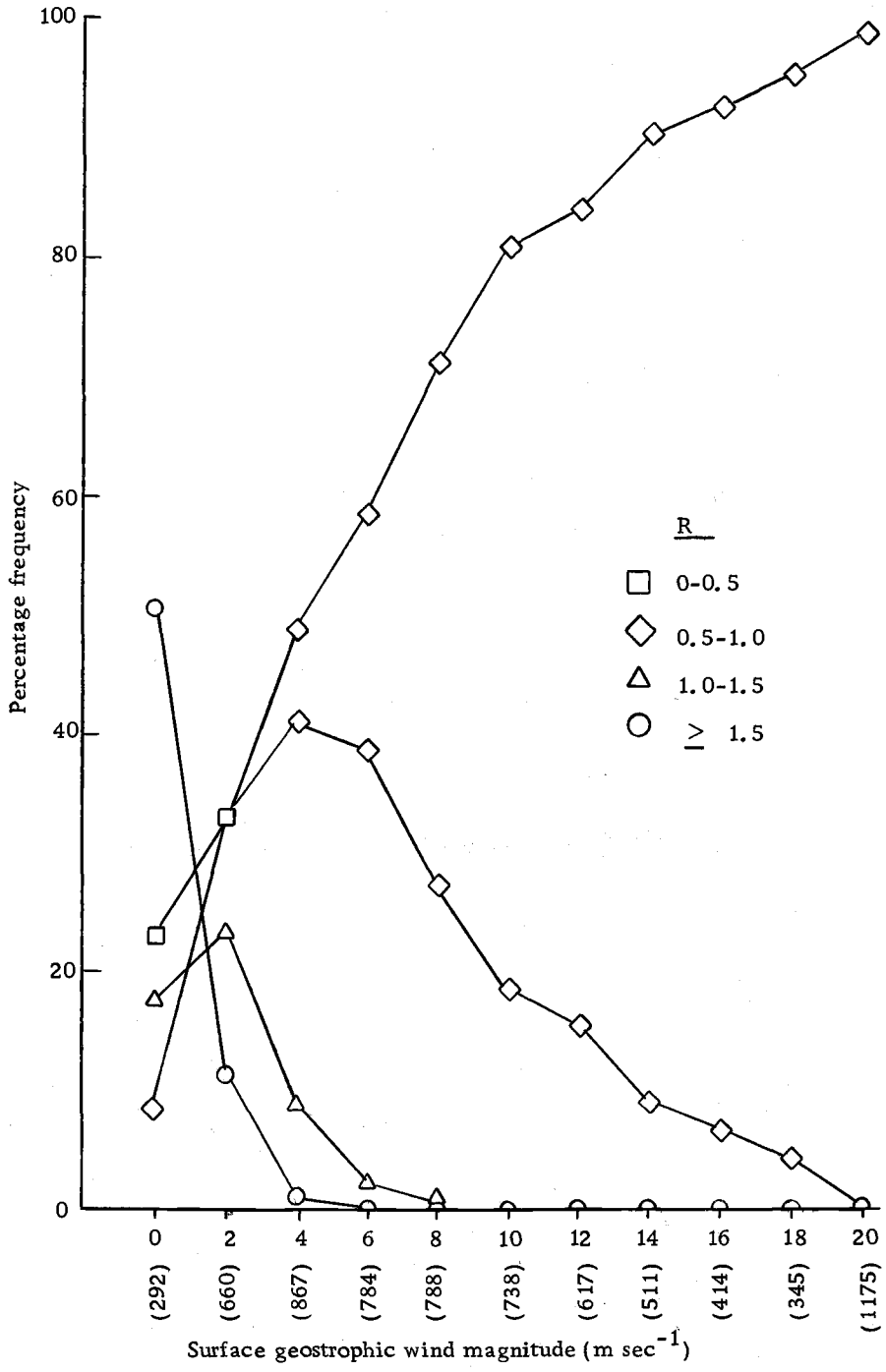

Figure 18. R frequency of selected surface geostrophic wind magnitude categories.

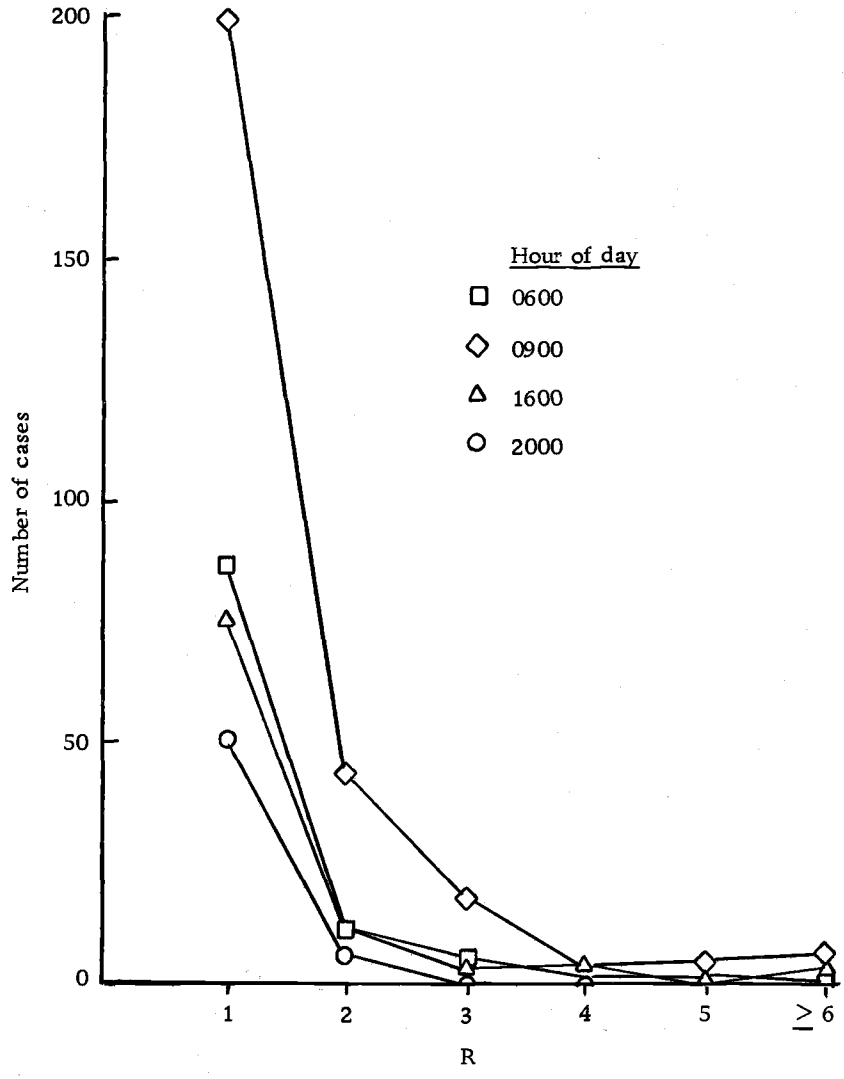

Figure 19. Hourly supergeostrophic wind frequency.

nocturnal stability and 1600 when marine air penetration most frequently occurs and accelerations not associated with the synoptic-scale pressure gradient are at a maximum.

The equation relating the 0900 summertime pressure gradient with the surface wind speed is:

$$\text{wind speed} = 1.56G - 0.10G^2 \qquad (11)$$

where G is as defined above. As in the wintertime cases, the results of the F-test show that these equations have low statistical significance.

The Cross-Valley Flow Situation

When the surface geostrophic wind has a cross-valley component the surface wind is still most frequently parallel to the valley and in the direction of the pressure gradient, again reflecting the strong dependence of α_o on the surface geostrophic wind relative to the valley. The angle α_o is negative in about 25% of the cases (flow component against the pressure gradient). Furthermore, α_o is most variable with moderate or strong westerly geostrophic flow. This is likely attributed to cases when air in the valley is stable in which case flow adjustment to the pressure gradient is slow.

Pressure gradients are weakest when the surface geostrophic wind is easterly. As a result, light small scale winds may be important.

The greatest variation and largest supergeostrophic values occur when the surface geostrophic wind is oriented across the valley. According to Munn (1966) this variation is the result of changes in the downward transport of turbulent east-west momentum. Pressure adjustments due to terrain may also be important.

The variations in downward momentum transport are dependent on stability. In winter relatively warm westerly surface winds rising over the Coast Range are forced to remain aloft due to cold air trapped in the Willamette Valley.

On the other hand, when surface flow from the Columbia Plateau is driven westward into the valley, instability frequently results. Vertical mixing transports momentum downward causing a more rapid adjustment of the surface flow to geostrophy.

VI. CONCLUSIONS

Surface wind direction in the Willamette Valley depends, of course, on the direction of the surface geostrophic wind. However, terrain features alter the standard surface wind-pressure gradient relationship such that the angle between the surface wind and surface geostrophic wind is typically much larger than that which would be expected over flat terrain. In one-fourth of the observations a component of the surface wind is against the pressure gradient estimated from synoptic observations. Perhaps this is partially due to the lack of resolution in determining the pressure field. Thus, terrain influences cause difficulties in accurately forecasting the surface winds from the synoptic-scale pressure gradient.

Stability also plays an important role in determining how accurately the surface winds may be predicted by the pressure gradient. With strong stability, terrain effects seem most important, complicating the relationship of wind to synoptic-scale pressure gradients. With weaker stability or surface heating the influence of terrain is reduced but still important.

The lack of predictability of surface winds seems to indicate that atmospheric air pollution models will have difficulty in accurately forecasting flow patterns in mountainous terrain. In particular under stable conditions, when the air pollution potential is greatest, surface

winds are hardest to predict.

In passing it is noteworthy to mention that the conventional operational technique of fitting the pressure field to the wind field in an attempt to forecast the surface wind from the synoptic-scale surface geostrophic flow frequently appears to be unsuited to mountainous terrain because of the importance of topography and meso-scale events. Improvements could be made by dividing data into several frequently occurring flow situations based on stability and the synoptic situation and regression equations for each flow situation calculated. However, the equations thus calculated would not be useful when meso-scale events were important.

BIBLIOGRAPHY

Aeronautical Chart and Information Center (U.S. Air Force). 1970. Jet navigation chart, JN-29N (17th ed.). Scale 1:2,000,000. St. Louis, Missouri.

Bernstein, Abram B. 1973. Some observations of the influence of geostrophic shear on the cross-isobaric angle of the surface wind. Boundary-Layer Meteor., 3, 381-384.

Cramer, Owen P., and Robert E. Lynott. 1961. Cross-section analysis in the study of windflow over mountainous terrain. Bull. Amer. Meteor. Soc., 42, 693-702.

Deacon, E.L. 1973. Geostrophic drag coefficients. Boundary-Layer Meteor., 5, 321-340.

Frenzel, Carroll W. 1962. Diurnal wind variations in central California. J. Appl. Meteor., 1, 405-412.

Haltiner, George J., and Frank L. Martin. 1957. Dynamical and Physical Meteorology. New York, McGraw-Hill. 454 pp.

Hasse, Lutz. 1974. Note on the surface-to-geostrophic wind relationship from observations in the German bight. Boundary-Layer Meteor., 6, 197-201.

Hewson, E. Wendell. 1964. Industrial Air Pollution Meteorology. Corvallis, Oregon, O.S.U. Bookstores, Inc. 191 pp.

_____ 1972. Personal communication.

Holzworth, George C. 1972. Mixing height, wind speeds, and potential for urban air pollution throughout the contiguous United States. Environmental Protection Agency, Office of Air Programs. 118 pp.

Hoxit, Lee R. 1974. Planetary boundary layer winds in baroclinic conditions. J. Atmos. Sci., 31, 1003-1020.

MacHattie, L.B. 1968. Kananaskis valley winds in summer. J. Appl. Meteor., 7, 348-352.

Melgarejo, J. W., and Deardorff, J. W. 1974. Stability functions for the boundary-layer resistance laws based upon observed boundary-layer heights. J. Atmos. Sci., 31, 1324-1333.

Munn, R. E. 1966. Descriptive Micrometeorology. New York, Academic Press. 216 pp.

Olsson, Lars E., Wesley L. Tuft, William P. Elliot, and Richard Egami. April 1971. A study of the natural ventilation of the Columbia-Willamette Valleys: II. Technical Report 71-2, Departments of Atmospheric Sciences and Oceanography and the Air Resources Center, Corvallis, Oregon. 164 pp.

Panofsky, Hans, and Glenn W. Brier. 1958. Some Applications of Statistics to Meteorology. University Park, Pennsylvania, The Pennsylvania State University. 208 pp.

Remington, Richard D., and M. Anthony Schork. 1970. Statistics with Applications to the Biological and Health Sciences. Englewood Cliffs, New Jersey, Prentice-Hall, Inc. 351 pp.

Taylor, G. I. 1916. Proc. Royal Soc. (London), A, 92.

Thompson, Rory O. R. Y. 1974. The influence of geostrophic shear on the cross-isobaric angle of the surface wind. Boundary-Layer Meteor., 6, 515-518.

APPENDIX

APPENDIX I

Deacon (1973) observed relationships between R and α_o for a five year period in the gently rolling countryside of the Salisbury Plain in southern England. Results are summarized in Table 2. The first column gives the set number. The second column lists season, hours of observation and the amount of sky cover. For each set and geostrophic wind category, the first row gives mean R values in percent. In the next line the number of observations appears to the left of the solidus and the standard deviation to the right. Mean α_o values are listed in the third row.

Comparisons between the flow above this English countryside and the Willamette Valley illustrate terrain influences. Above the plain the largest α_o and smallest R values occur in the early morning hours (Sets VII and VIII) when stability is greatest. In the early afternoon during the summer, R is large and α_o is small. The importance of surface heating is shown in Sets I through III. With increasing cloudiness surface flow is increasingly decoupled from the geostrophic flow. As a result, R decreases and α_o increases. In the Willamette Valley, the largest α_o and smallest R values also occur in the early morning hours. However, throughout the entire year α_o is most frequently 60° as surface flow is channeled parallel to the valley. Furthermore, early afternoon R

in the summer is one-third of that above the English plain. Evidently surface flow in the Willamette Valley cannot adjust as rapidly as the pressure gradient intensifies.

Table 2. Observed values of R and α_o above gently rolling terrain (after Deacon, 1973).

Set No.		G(m s^{-1}) 3	6	8	10	12.5	15	20	25	30
I	Summer; 12-15h	83	72	72	70	-	-	-	-	-
	nil-3/10	5/-	7/15	12/11	5/-	-	-	-	-	-
				21						
II	Summer; 12-15h	66	74	71	67	74	60	60	-	-
	4/10-7/10	6/21	20/19	15/15	8/15	9/12	9/13	7/10	-	-
				31			35			
III	Summer; 12-15h	-	76	68	62	67	67	50	-	-
	8/10-10/10	-	22/22	25/15	20/16	17/14	6/15	22/11	-	-
				35			31			
IV	Equinoctial; 12-15h	73	67	70	59	57	51	-	-	-
	nil-3/10	8/26	14/18	12/23	10/15	10/12	5/-	-	-	-
				32			29			
V	Equinoctial and winter day	65	57	51	50	51	47	43	41	38
	8/10-10/10	23/29	36/22	73/16	77/16	80/14	33/11	118/9	25/8	19/5
		40		39			33		29	
VI	Winter; 12-13h	-	-	56	56	52	-	-	-	-
	nil-3/10	-	-	5/-	8/-	5/-	-	-	-	-
				24			29			
VII	All seasons, 03h	36	35	38	36	38	38	38	38	-
	and winter, 06h	31/21	51/15	48/16	46/11	50/13	15/10	34/13	4/-	-
	nil-3/10	54		52			44		37	
VIII	All seasons, 03h	54	43	45	44	46	44	42	36	42
	and winter, 06h	29/24	51/18	69/14	52/22	73/13	41/10	106/12	32/15	9/10
	8/10-10/10	53		48			37		30	